231

Reprinted from JOURNAL OF THE ATMOSPHERIC SCIENCES, Vol. 49, No. 15, 1 August 1992
American Meteorological Society

Observations of Cloud-Top Entrainment in Cumuli

JEFFREY L. STITH

Observations of Cloud-Top Entrainment in Cumuli

JEFFREY L. STITH

University of North Dakota, Grand Forks, North Dakota

(Manuscript received 25 March 1991, in final form 11 November 1991)

ABSTRACT

Sulfur hexafluoride tracer gas was released during single aircraft passes just above growing convective turrets to study its entrainment into the clouds as they grew through the release altitude. The tracer was sampled in situ from a second research aircraft that carried a real-time sulfur hexafluoride analyzer. The results from three experiments are presented. They were done with clouds ranging in size from a vigorous convective turret to a small cumulus.

The observations suggest that during the early stages of entrainment, the tracer remained mostly out of the cloud and was carried alongside the upper cloud regions by the circulation present there. In each experiment, concentrated tracer was first found on the edges of the turrets. Later, the tracer mixed into the central portions of the turrets where it had diluted considerably and mixed through most of the turret. The observations are consistent with the hypothesis that cloud-top entrainment occurs through a vortex-like circulation that brings air from above the cloud into the central region of the cloud. The results are compared to some recent conceptual and numerical models of entrainment.

1. Introduction

Much of the progress in understanding entrainment has been due to new approaches in analyzing thermodynamic data or on progress in the refinement of various numerical models. Thermodynamic techniques may be used to determine the origin of entrained air (e.g., Paluch 1979; Boatman and Auer 1983) but are limited by our ability to measure humidity or temperature, especially on small scales. Numerical models simulate the history of cloudy or entrained air parcels (e.g., Reuter and Yau 1987), but observational techniques have not been available to provide comparable information for natural clouds.

In this study I report on the first experiments to use a tracer, sulfur hexafluoride (SF_6), to tag the air above growing cumuli and to observe its entrainment into the cloud and the subsequent evolution of the entrained air. The tracer was released during single aircraft passes just above the tops of growing convective turrets and was sampled by a research aircraft as the tops of the clouds grew into the release altitude. These techniques and the results of three experiments are described below.

2. Experimental methods and instrumentation

Sulfur hexafluoride is a nonnaturally occurring tracer that is insoluble in water and easily detectable at ten parts per trillion levels in the atmosphere. It is inert and inexpensive and has been used as a tracer for many years in air quality studies. It was released in a gaseous form by a treatment aircraft at a rate of approximately 0.5 kg km^{-1}. The releases were started as the treatment aircraft approached a growing convective turret that was to be the candidate cloud and ended after the aircraft had passed over the turret. Therefore, the initial tracer distribution was a narrow plume of tracer above the growing turret that extended well outward of the cloud region on both sides.

During the treatment pass a research aircraft, the University of North Dakota Citation, followed the treatment aircraft. The Citation followed just behind and below to maintain visual contact with the upper aircraft until the Citation entered the cloud. If the cloud exhibited strong updraft during the treatment pass, the next sampling pass was made at a higher altitude, just below the release altitude. For clouds that did not appear to be growing, the next passes were made at an altitude that would place the Citation within about 300 m of the estimated visual cloud tops. The release and sampling methods are illustrated in Fig. 1.

A real-time "pointer"-type system was employed to assist in guiding the Citation back to the location of the cloud. The pointer displays heading, distance, elapsed time, and altitude required to intercept a parcel of air assumed to be advected with the measured wind field. Up to three pointers can be set and followed on the Citation's data system. During the treatment pass the pointers were set as updrafts were encountered in the central cloud region or in areas of relatively high concentrations of liquid water. The pointer that was set in the most vigorous (highest updraft or liquid water) cloud region during the treatment pass was fol-

Corresponding author address: Dr. Jeffrey L. Stith, Department of Atmospheric Sciences, Box 8007, University Station, Grand Forks, ND 58202.

© 1992 American Meteorological Society

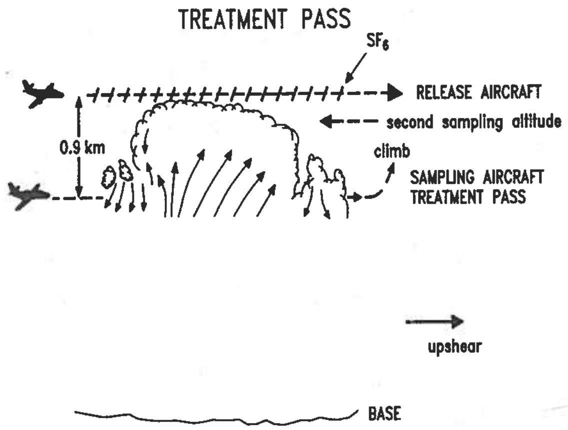

FIG. 1. Diagram of the aircraft sampling and treatment experiment as applied to the cloud on 22 June 1989. See text for more details.

lowed until intercept of the tracer. This proved to be a successful method of staying with the candidate turret (which was often part of many nearby turrets) until the tracer was found. Once it was detected, the pointer was updated at the tracer location on each successive pass. Since the time required to return to the cloud following a pass was about 2 min, this allowed the pointer to be updated at this rate. These and previous studies (e.g., Stith et al. 1990) suggest that this update rate is generally adequate to follow tracer releases in convective clouds horizontally, but the vertical component often diverges from the tracer location in vigorous clouds due to vertical accelerations.

The Citation carried a fast-response (with about a 1-s response time) analyzer for SF_6 of a type described by Benner and Lamb (1985). More information on the performance of the analyzer for this application is given in Stith and Benner (1987). Other instrumentation included a number of standard instruments for wind and microphysical measurements. These included an inertial navigation and gust probe system for wind and turbulence measurements, an NCAR-type reverse-flow temperature sensor, a Cambridge System–design dewpoint hygrometer, and pressure transducers for measurement of static and Pitot pressures. Particle Measuring Systems (PMS) probes (FSSP, 1DC, 2DC, 1DP) were used for microphysical measurements.

PMS data were recorded at 4 Hz and the other measurements were recorded at 24 Hz. The FSSP data were corrected for sizing and concentration errors incurred by optical coincidence and electronic dead time as described by Baumgardner et al. (1985).

Liquid water concentrations were computed from the corrected FSSP data. As a check on the performance of this method, the liquid water measurements were compared against adiabatic values from a cloud that occurred on 28 June 1989 during the 1989 North Dakota Thunderstorm Project (Boe et al. 1992). Several cloud passes were made in a developing cloud region that exhibited large (greater than 2 km) adiabatic regions, based on a comparison of cloud-base measurements of temperature and pressure from a second aircraft (the University of Wyoming King Air) with in-cloud measurements of temperature and pressure from the Citation that were obtained at cloud midlevels. The cloud was nonprecipitating (in the adiabatic regions). It was also supercooled at the sampling level of the Citation, so wetting effects (Lawson and Cooper 1990) on the reverse flow temperature sensor were minimized. In these regions, the FSSP liquid water measurements were within 10% of the computed adiabatic value, which is reasonably good agreement given the difficulties involved in this type of measurement.

The aircraft made soundings from the sampling levels to well below cloud, usually en route to the candidate cloud or during the return from the cloud. These were used to estimate the height of cloud base and the adiabatic liquid water content at the sampling altitudes.

The sampling procedures were intended to follow that portion of the initial tracer plume that was affected by the cloud circulation and interacted with the cloud. These regions were initially only a few hundred meters across (about 3 s of sampling time) but could be sampled repeatedly by referencing the pointer system as the cloud evolved. However, on these scales it is impossible to determine what part of the region (its center or edge) is being sampled. Thus, the observed maximum SF_6 concentrations represent lower limits to the actual maximum concentrations, especially in the early stages of sampling when the tracer region is small. For some of the experiments, orthogonal sampling passes were made to better define the horizontal extent of the tracer.

In a slightly different experiment, Stith and Politovich (1989) followed a similar release of SF_6 made at the base of a small cumulus. After it had come to rest near the top of the cloud, sequential passes through the tracer produced patterns of similar concentration profiles, which suggests that the sampling in that experiment may have been more successful at mapping out the tracer than it is in the more rapidly evolving situation in these experiments. They estimated the subsequent dilution of the region by assuming that representative samples of the SF_6 region were obtained. This assumption is probably less valid for the cases presented here.

Even with the above limitations, the tracer experiments provide positive identification of entrained air regions and identify their original altitude. Since the treatment aircraft is over the top of the turret for less than 1 min, the time the air was at the release point is reasonably well determined. This is a great help in constructing a history of the region as it is entrained by the cloud.

3. Results

The results from three experiments are presented below. The most vigorous convective system occurred

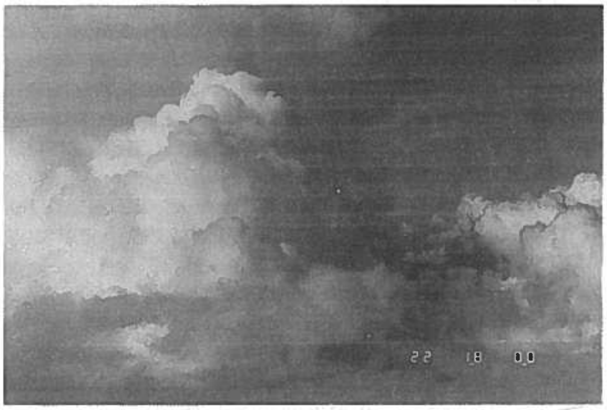

FIG. 2. The region treated on 22 June 1989. The photograph was taken towards the north-northeast approximately 3 min prior to the start of treatment.

on 22 June 1989 during the North Dakota Thunderstorm Project. The experiment was conducted on a turret that was part of a larger precipitating cumulonimbus. The two other cases were from smaller clouds that occurred on 11 August 1990 in central Illinois.

a. Vigorous convection: 22 June 1989

The cloud system investigated was a small-to-moderate–sized cumulonimbus that occurred about 150 km west of Bismarck, North Dakota. The cloud region selected for treatment was an isolated turret that visually appeared to be growing vigorously. An older glaciated region of the cloud was above and just north to northeast of the treated turret. The developing turret and glaciated region are evident in a photograph taken at 1800 (LST) approximately 3 min before the start of treatment (Fig. 2).

A sounding taken outside the cloud is presented in Fig. 3. Cloud base was not measured but was estimated to be at 2.5 km (MSL: 750 mb), near the level of free convection and the LCL for subcloud air. An inversion was present at 680 mb; once the cloud had risen above that level, the atmosphere was very dry but had a nearly moist adiabatic lapse rate outside of the cloud, suggesting that the buoyancy of a rising cloud parcel would be nearly constant above that level. The cloud growth was probably limited by an inversion above 490 mb.

Treatment was done at 6.1-km altitude (MSL, pressure altitude, 470 mb), with the Citation following just behind and below at 5.2 km (pass 1) in a southeasterly direction nearly parallel to the wind direction from 320 deg. Most of the horizontal wind shear was speed shear, with light winds of 2.5 m s^{-1} at the sampling altitudes and twice that at the cloud base, which provided light wind shear (with upshear on the southeastern side of the cloud). Comments from the flight crew indicated that they remained above the turret during the pass, except for a brief moment when the aircraft entered the very summit of the turret.

After the treatment pass (pass 1), the Citation ascended to 5.8 km and made three passes (passes 2–4) in a direction that alternated between along and orthogonal to the treatment axis. The final pass (pass 5) was made at 5.5 km along the treatment axis. A schematic of the flight path (relative to the cloud) and the cloud and tracer locations is shown in Fig. 4, along with the beginning and end times of 1-min passes through the cloud.

The results from the aircraft measurements made during passes 1–5 are presented in Figs. 5, 6, and 7. During pass 1 (Fig. 5) the turret had a warm, positively buoyant updraft that covered the main cloudy region. Cooler, negatively buoyant downdrafts were found on both sides of the updraft. The gust data indicate that the in-cloud motion had a southerly component, suggesting that the updraft retained some of the momentum it had when it was lower. The gust data from the northern downdraft region (the downwind/downshear side) indicated a divergent flow. The northern downdraft contained only traces of cloud drops, while the southern downdraft had only slightly more drops. This suggests that these were evaporating cloud regions.

During pass 1 the updraft contained small (200-μm diameter) ice particles in relatively low concentrations (Fig. 5). On subsequent passes the cloud region glaciated considerably (Figs. 6 and 7). During pass 1 the liquid water concentrations were close to adiabatic in the central part of the turret. The drop sizes were also very uniform across this region. Thus, at the time of treatment, the cloud consisted of a central updraft region containing cloud-base air without significant entrainment, surrounded by narrow downdrafts of evaporating cloud.

Pass 2 was roughly perpendicular to pass 1 and was on the northern edge of the turret sampled during pass

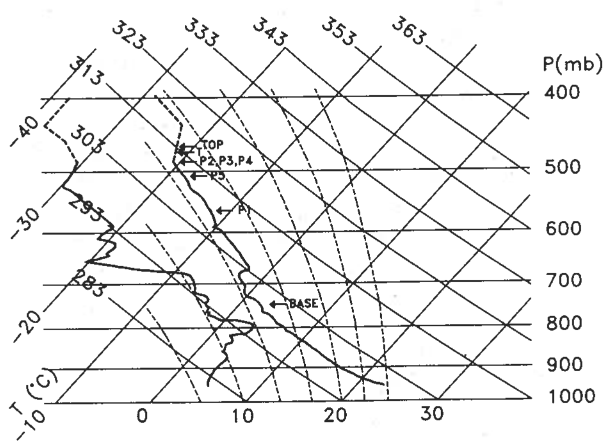

FIG. 3. The results from an aircraft sounding made during the return to Bismarck between 1908 and 1930 LST 22 June. Some additional data from a balloon sounding at Bismarck at 1900 is represented by the dashed line. The altitudes of the Citation during each of the sampling passes is indicated as P1, P2, P3, P4, P5, for passes 1 through 5, respectively. The altitude of treatment is indicated as T on the sounding.

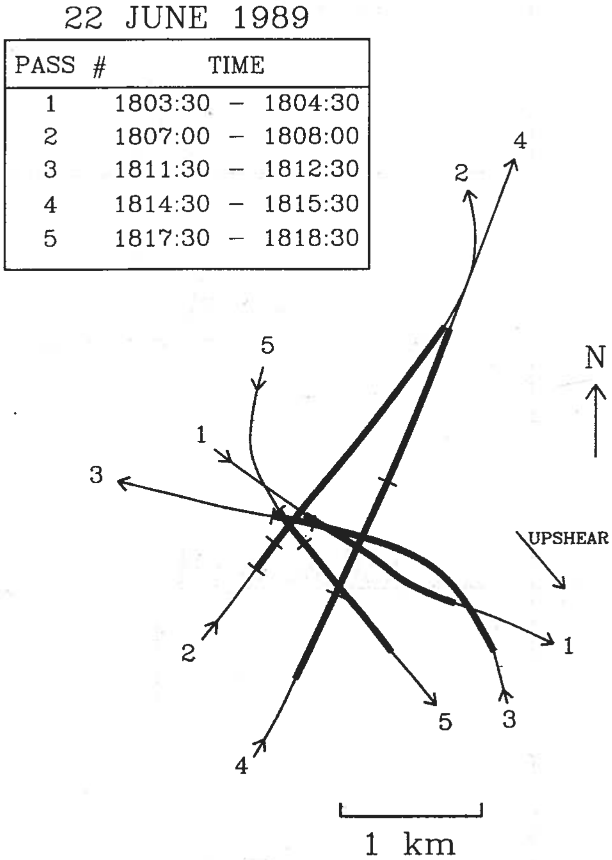

FIG. 4. Plan view of the Citation flight track on 22 June 1989 relative to the cloud. Cloud motion was based on the measured horizontal winds at the sampling altitude. The cloud location is indicated by the thick portion of each line. The tracer material was detected between the locations marked by the small lines perpendicular to the flight track. Pass numbers are given at the end of each track segment. The time of each pass to the nearest 1-min segment is given.

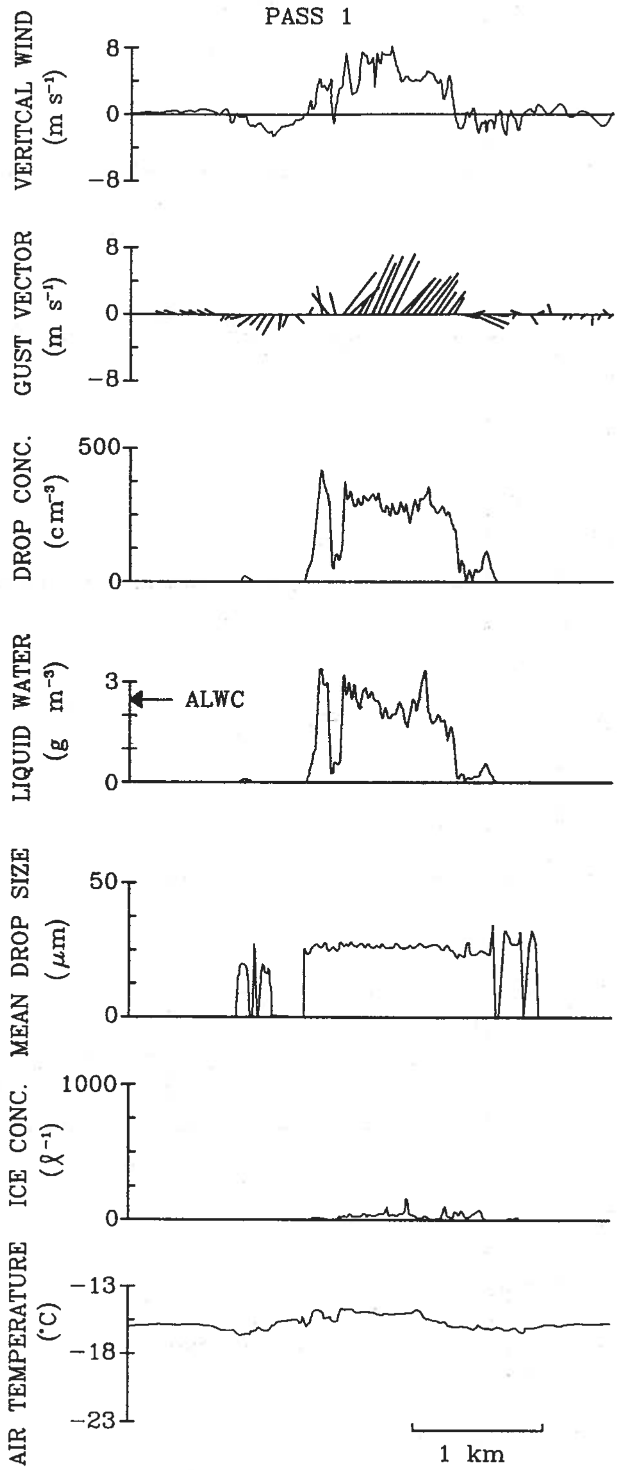

FIG. 5. Vertical wind, gust vector (turbulent air motion in the vertical plane of the aircraft), droplet concentration, liquid water content, volume mean droplet size, ice concentration (from the 2DC shadow or count), and reverse-flow air temperature for the treatment pass (pass 1). The droplet and liquid water data are from an FSSP probe. The estimated adiabatic liquid water content is indicated by the arrow by ALWC. For the gust vector, the length of each line represents speed (corresponding to the scale at the left), while the direction of the line indicates the gust direction in the vertical plane of the aircraft.

1 (Fig. 4). This led into the large glaciated region of cloud to the northeast of the treated turret. The tracer was found in a weak downdraft region located in the vicinity of the downshear/downwind region of pass 1. Small amounts of cloud liquid water and ice were found with the tracer, although neither the tracer or cloud filled the downdraft region. The downdraft region had a temperature similar to that in the environment.

The strongest tracer concentrations were found during pass 3 on the northern side of the cloud (Figs. 4 and 6). The turret had a similar structure to that observed during pass 1, except that it had mostly glaciated and the updraft and buoyancy had decreased. The narrow tracer region was about half in and half out of the updraft. The gust data in this region revealed a pattern that resembled a small vortex (see the arrow in Fig. 6, pass 3). This was clearly moving the tracer toward the cloud.

During pass 4, 3 min later, the aircraft went through the central portion of the turret region and probably also hit part of the older cloud region in the later half of the pass (Figs. 4 and 7). The tracer now covered a

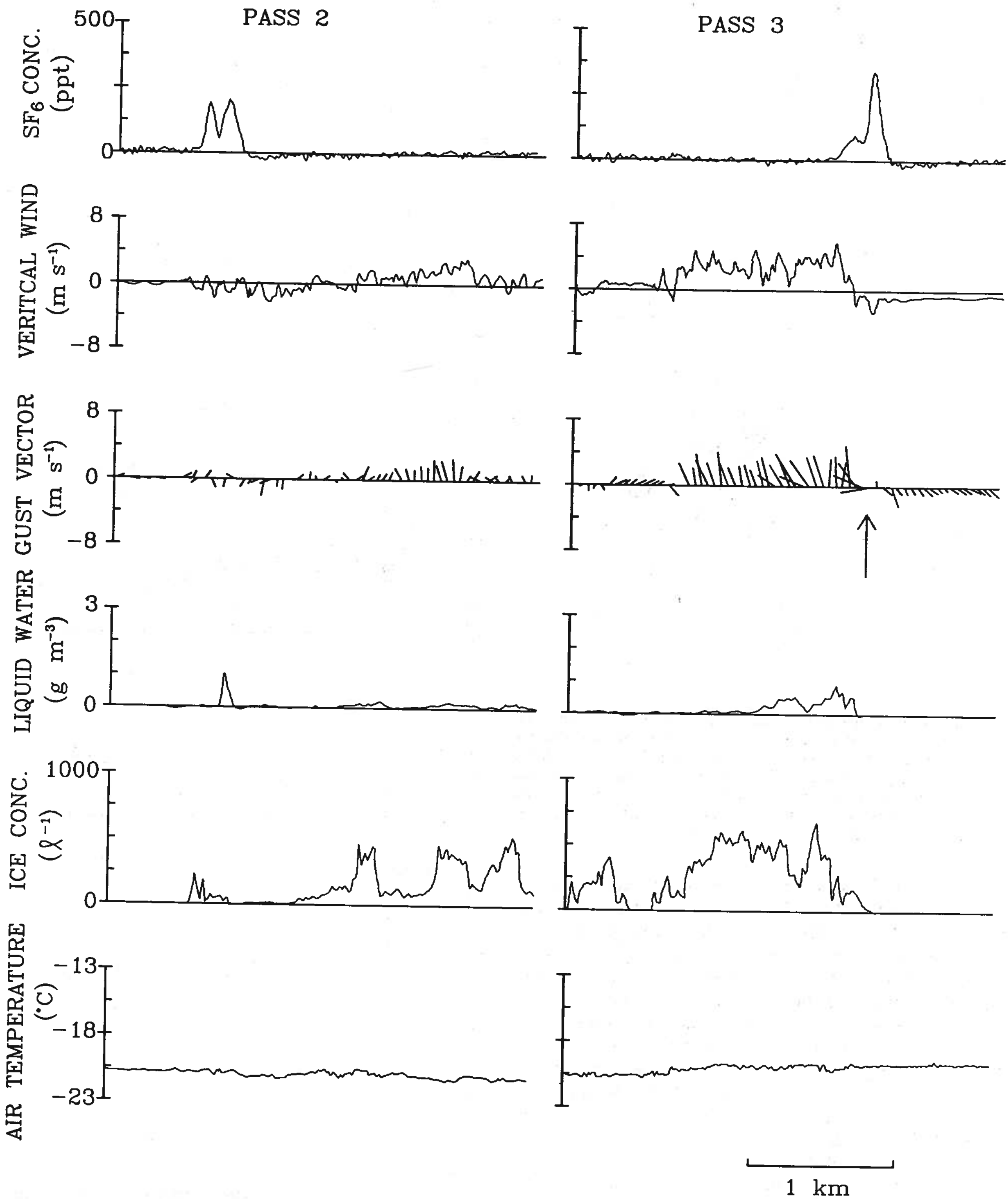

FIG. 6. As in Fig. 5 except for SF_6 concentration, vertical wind, gust vector, liquid water content, ice concentration, and reverse-flow temperature for passes 2 through 5. A small vortex-like region is indicated by the arrow in pass 3.

much larger region but at a much lower concentration, suggesting that considerable dilution had occurred during the 4-min period between passes 3 and 4. Both updraft and downdraft regions were now evident in the region of the cloud containing the tracer, but mild updraft regions covered more of the cloud. The largest

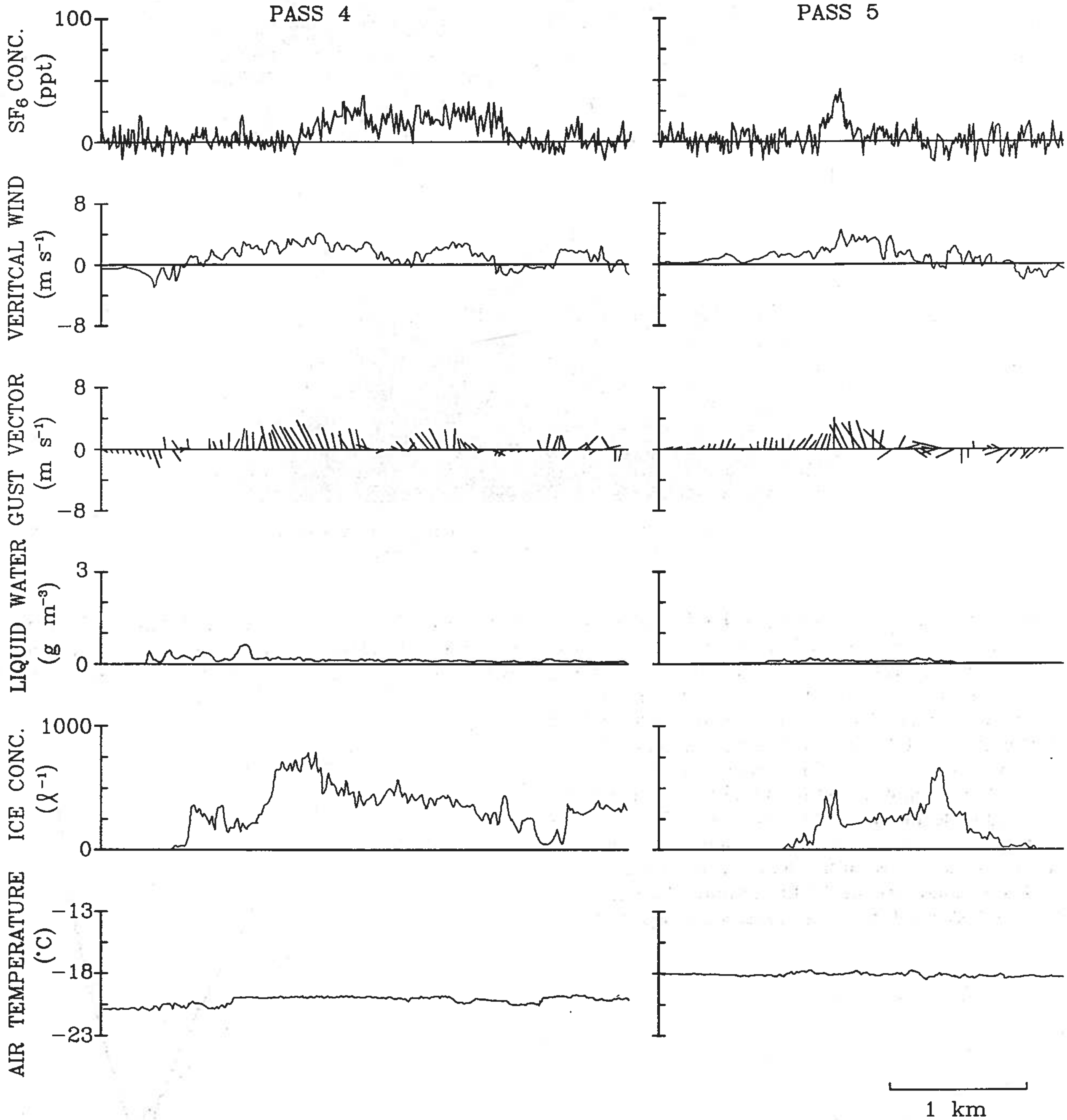

FIG. 7. As in Fig. 6 except for passes 4 and 5. (Note the change in scale for SF_6 concentration.)

area of updraft, on the west side of the cloud, was also still buoyant, suggesting that the cloud was still somewhat active.

During pass 5 a small dilute tracer region was found in a weak updraft near the location where it was observed earlier in passes 2 and 3 (Figs. 4 and 7).

b. Intermediate-sized convection on 11 August 1990

A smaller and more isolated convective cloud was sampled on 11 August 1990. It was located 125 km northwest of Champaign, Illinois. Although a few precipitation-sized particles were eventually produced by the cloud, it dissipated before significant amounts of precipitation were produced. A photograph of the cloud, obtained about 4 min prior to treatment, is provided in Fig. 8.

A sounding taken just after sampling while returning to Champaign is presented in Fig. 9. The estimated visual cloud tops at 5.0 km (540 mb) were capped by a small inversion. The observed lapse rate was nearly moist adiabatic below this inversion to about 3.0 km

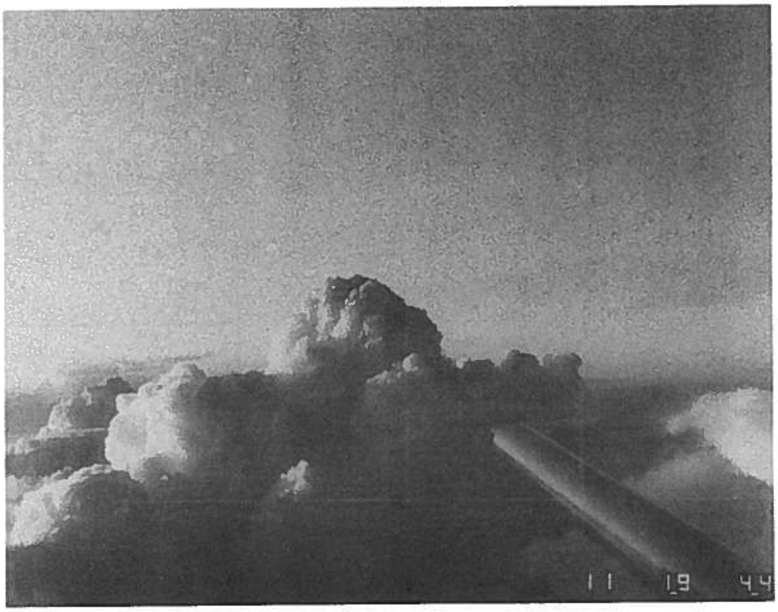

FIG. 8. Photograph of intermediate-sized convection on 11 August 1990 about 4 min prior to the start of treatment.

(700 mb), so it was likely that the cloud base extended down to about that level. Several layers of different stability were present below the cloud base, suggesting that the bottom of the convective layer was elevated from the surface. The cloud-top region was treated during pass 1 at 4.8 km. Sampling was conducted at 4.5 km (pass 1) and 4.8 km (passes 2 and 3), so the cloud depth below the sampling altitude was similar but slightly less than the 22 June cloud. However, unlike the 22 June case, the atmosphere was near saturation through most of the depth of the cloud.

Below cloud base at 2.8-km altitude the wind was from 310 deg at 6 m s^{-1} and increased slightly to 10 m s^{-1} from 275 deg at 3.5 km and was steady from there up to the cloud top. Thus, there was weak shear (with upshear to the southwest) at lower levels of the

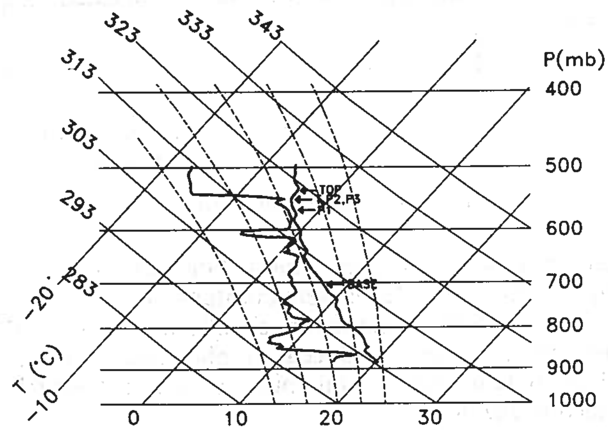

FIG. 9. The results from an aircraft sounding made during the return to Champaign between 2020 and 2035. The altitudes of the Citation during each of the sampling passes is indicated as P1, P2, P3, for passes 1 through 3, respectively. The altitude of treatment is indicated as *T* on the sounding.

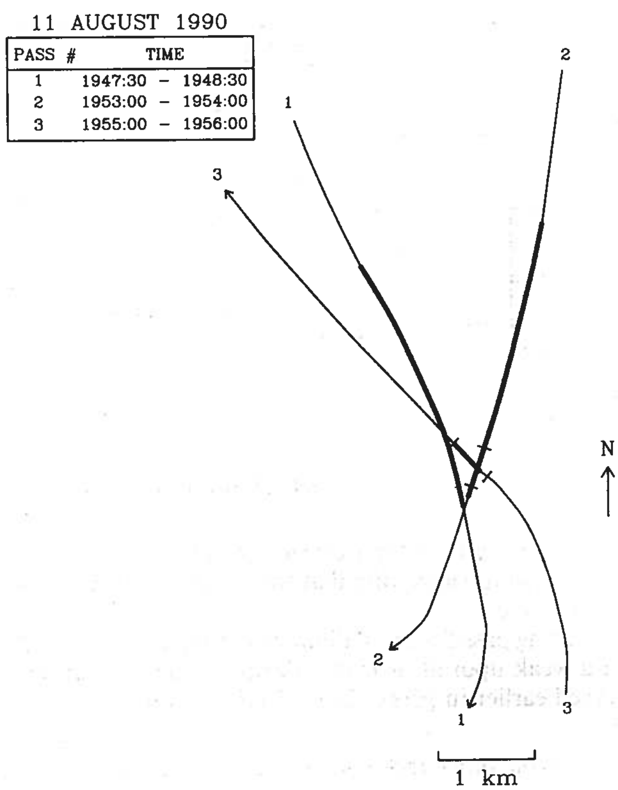

PASS #	TIME
1	1947:30 – 1948:30
2	1953:00 – 1954:00
3	1955:00 – 1956:00

FIG. 10. As in Fig. 4 except for the intermediate-sized cloud on 11 August 1990.

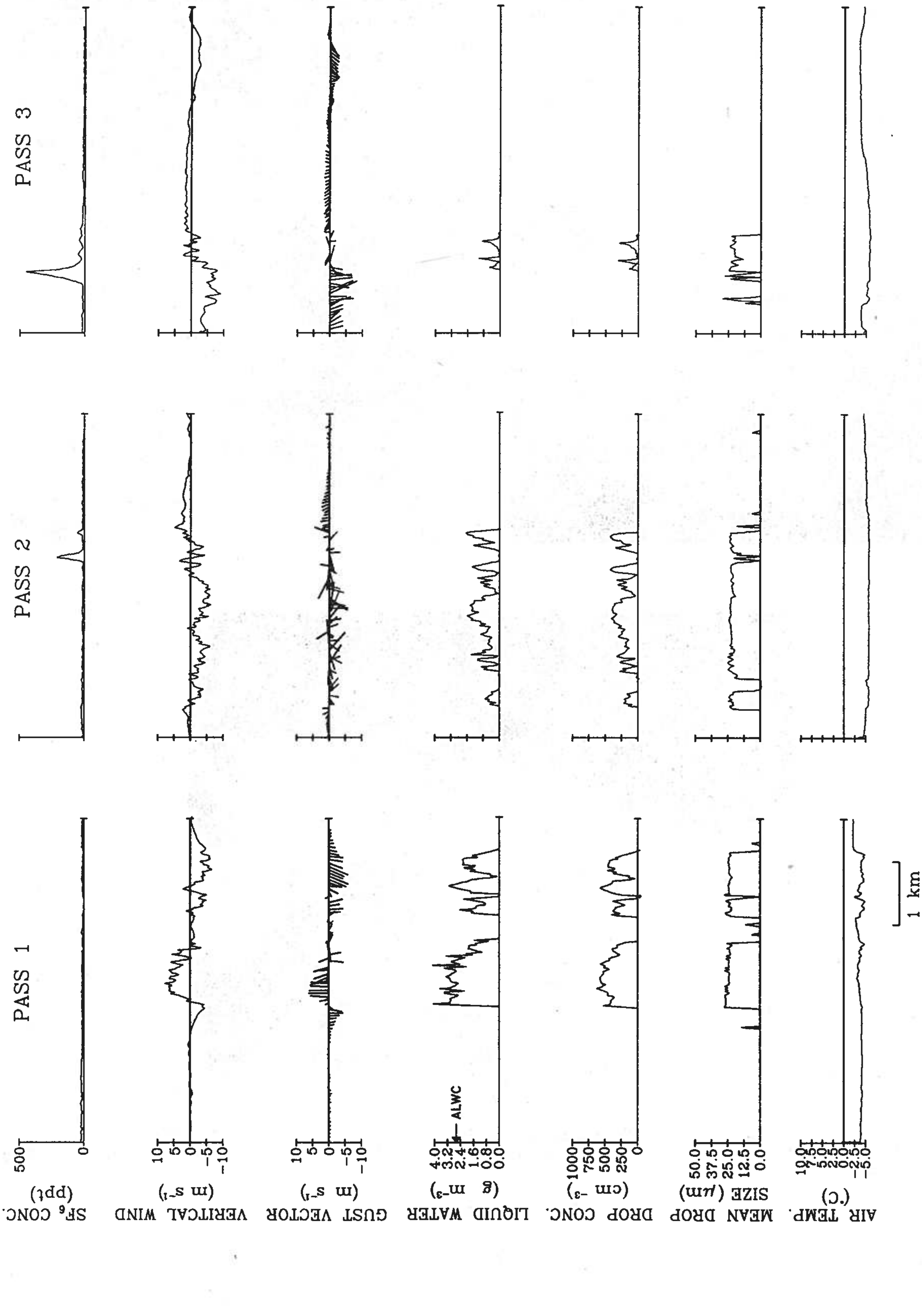

FIG. 11. As in Fig. 5 except SF_6 concentration, vertical wind, gust vector, liquid water, droplet concentration, volume mean droplet size, and air temperature for the intermediate-sized cloud on 11 August 1990. The data from the turret region selected for treatment is to the right of the largest cloud region evident in pass 1.

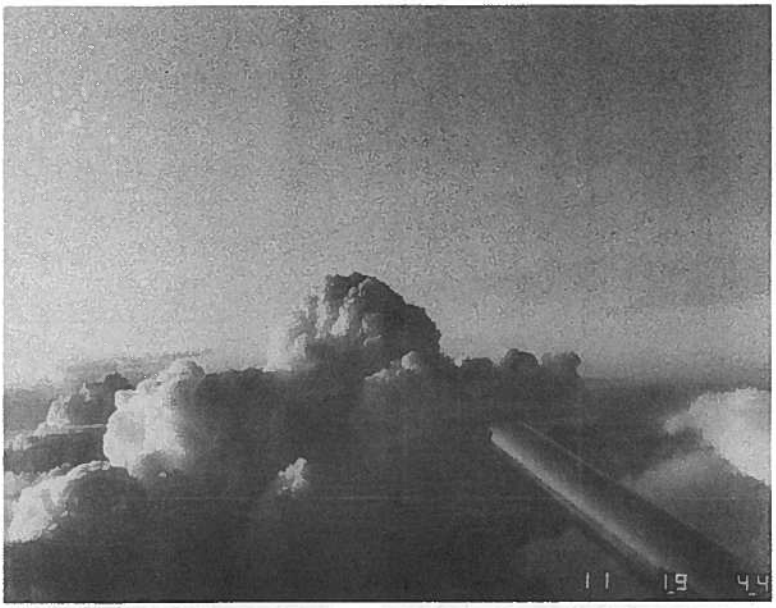

FIG. 8. Photograph of intermediate-sized convection on 11 August 1990 about 4 min prior to the start of treatment.

(700 mb), so it was likely that the cloud base extended down to about that level. Several layers of different stability were present below the cloud base, suggesting that the bottom of the convective layer was elevated from the surface. The cloud-top region was treated during pass 1 at 4.8 km. Sampling was conducted at 4.5 km (pass 1) and 4.8 km (passes 2 and 3), so the cloud depth below the sampling altitude was similar but slightly less than the 22 June cloud. However, unlike the 22 June case, the atmosphere was near saturation through most of the depth of the cloud.

Below cloud base at 2.8-km altitude the wind was from 310 deg at 6 m s^{-1} and increased slightly to 10 m s^{-1} from 275 deg at 3.5 km and was steady from there up to the cloud top. Thus, there was weak shear (with upshear to the southwest) at lower levels of the

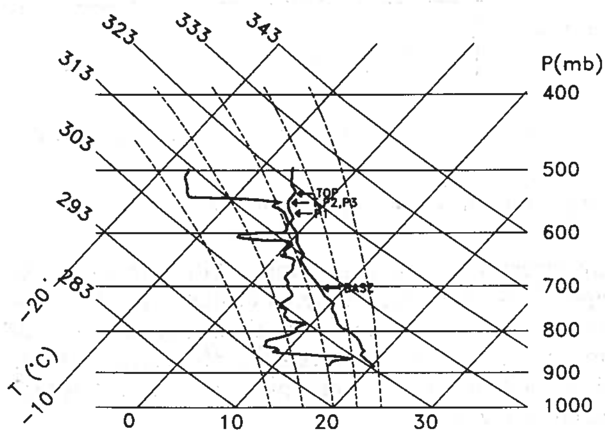

FIG. 9. The results from an aircraft sounding made during the return to Champaign between 2020 and 2035. The altitudes of the Citation during each of the sampling passes is indicated as P1, P2, P3, for passes 1 through 3, respectively. The altitude of treatment is indicated as T on the sounding.

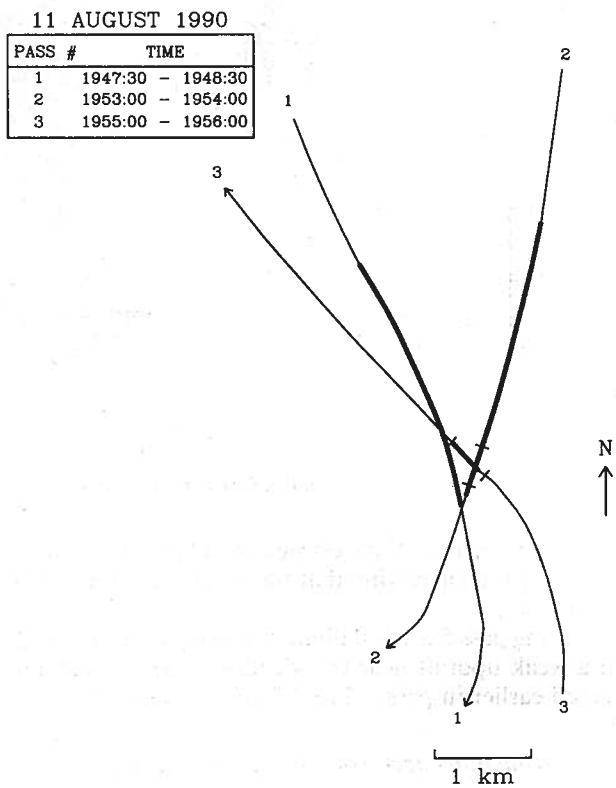

FIG. 10. As in Fig. 4 except for the intermediate-sized cloud on 11 August 1990.

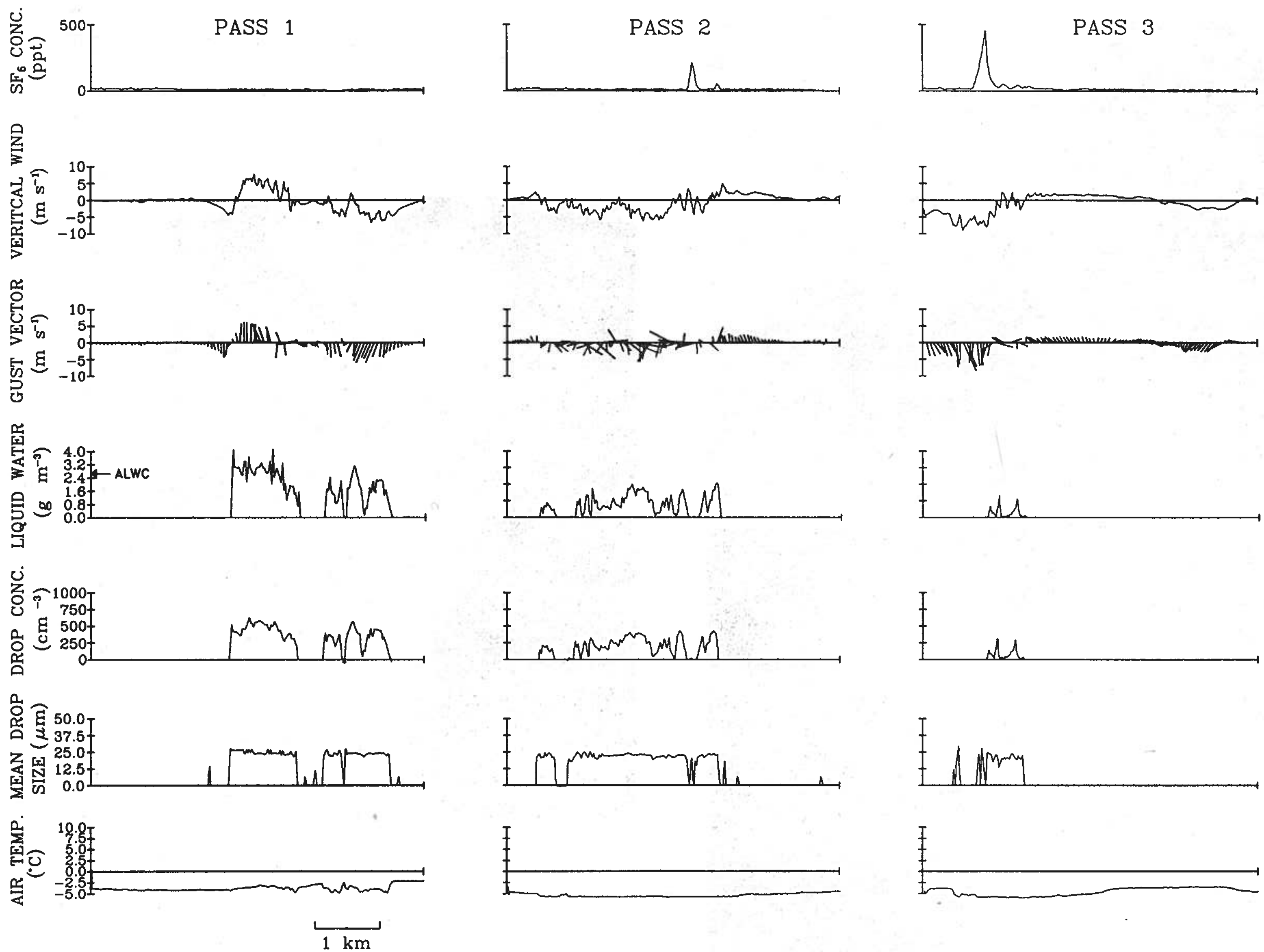

FIG. 11. As in Fig. 5 except SF_6 concentration, vertical wind, gust vector, liquid water, droplet concentration, volume mean droplet size, and air temperature for the intermediate-sized cloud on 11 August 1990. The data from the turret region selected for treatment is to the right of the largest cloud region evident in pass 1.

cloud but little shear in the vicinity of the sampling altitudes.

A treatment run (pass 1) and two subsequent passes were made through the cloud along a north–south axis (Fig. 10). The results are presented in Fig. 11. The treated turret was on the southern end of a more vigorous, larger cloud that is evident in Fig. 11. During treatment the central region of the cloud at 4.5-km altitude had almost stopped rising and was surrounded by cold, descending cloudy regions.

On the second pass, 300 m above the first, the cloud was more continuous, with most of the cloud region in downdraft, except for some small regions on the southern side of the cloud (Fig. 11) where the treated turret was located. The tracer was found on both edges of a small turret that was adjacent to the main cloudy region. The tracer had not mixed through the turret, but was confined to both edges.

On the third pass the highest tracer concentrations were still primarily on the edge of the turret, but small amounts of tracer had mixed through the cloud, which by now had begun to evaporate (Fig. 11, pass 3).

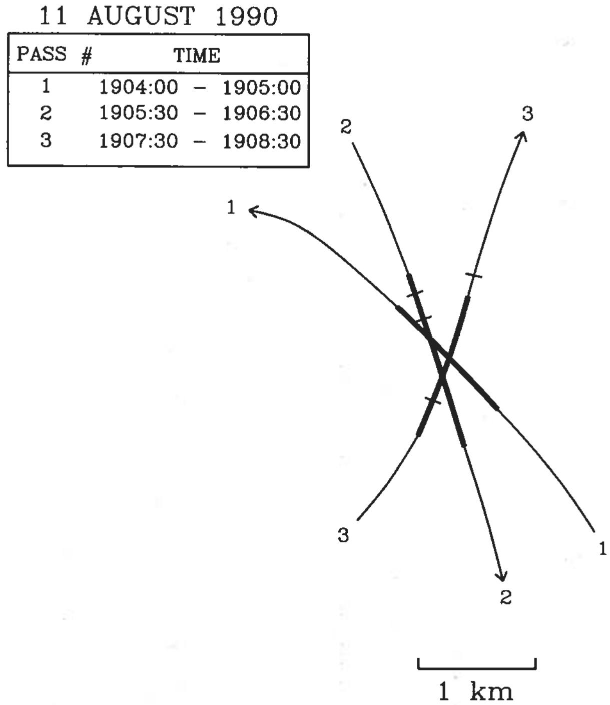

FIG. 14. As in Fig. 10 except for the small convective cloud on 11 August 1991.

c. *Small, nonprecipitating convection on 11 August 1991*

Earlier in the day an experiment was conducted on a smaller cloud that formed 25 km northeast of Champaign. Photographs of the cloud at various stages are given in Fig. 12. Eighteen minutes prior to treatment the area was part of a developing cumulus congestus region (Fig. 12a). As the aircraft approached the cloud for treatment, the convective activity in the area appeared to the flight crew to be diminishing, but the candidate turret still appeared to be growing with well-defined boundaries near the top (Fig. 12b). Cloud tops did not reach much above the treatment altitude of 3.6 km, due to the presence of a small inversion that is evident in the sounding made en route to the cloud from Champaign (Fig. 13). The cloud evidently did not have enough buoyancy to carry through this inversion and consequently must have started from about 710 mb (2.9 km).

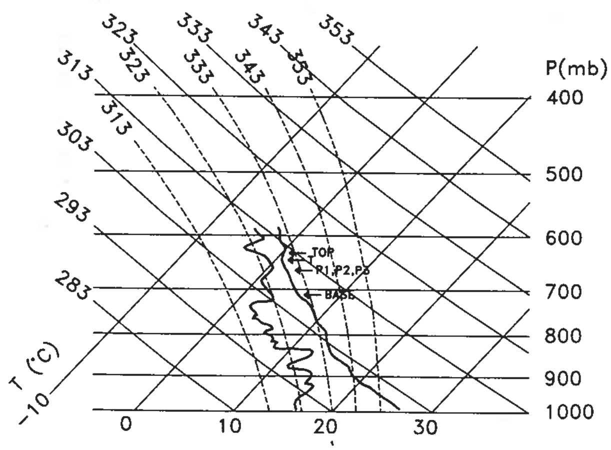

FIG. 13. As in Fig. 9 except taken between 1840 and 1845 while en route to the small convective cloud on 11 August 1991.

A treatment pass and two additional passes were conducted along a north–south orientation (Fig. 14). Since the cloud growth appeared to be subsiding, all the sampling passes were made at 3.3 km. The results are presented in Fig. 15. During the treatment pass the cloud contained a large downdraft on the southern part of the cloud and only a slight updraft on the northern edge of the cloud where the greatest liquid water concentrations (near adiabatic) were also observed. Only a slight downdraft was present outside the north edge of the cloud. On the second pass (Fig. 15, pass 2) the northern downdraft was more pronounced. The cloud now exhibited a weak central updraft surrounded by larger downdrafts. A high concentration of tracer was observed within the downdraft region on the north side, just alongside the cloud. Although the central portion of the cloud had some small areas of near-adiabatic liquid water, most of the cloud was subadiabatic. On the third pass the tracer was mixed through the northern two-thirds of the cloud region and was entirely in downdrafts. Observations from the flight crew indicated that the cloud top had descended to near the sampling altitude and that the cloud was dissipating at the time the photo in Fig. 12c was taken during pass 3.

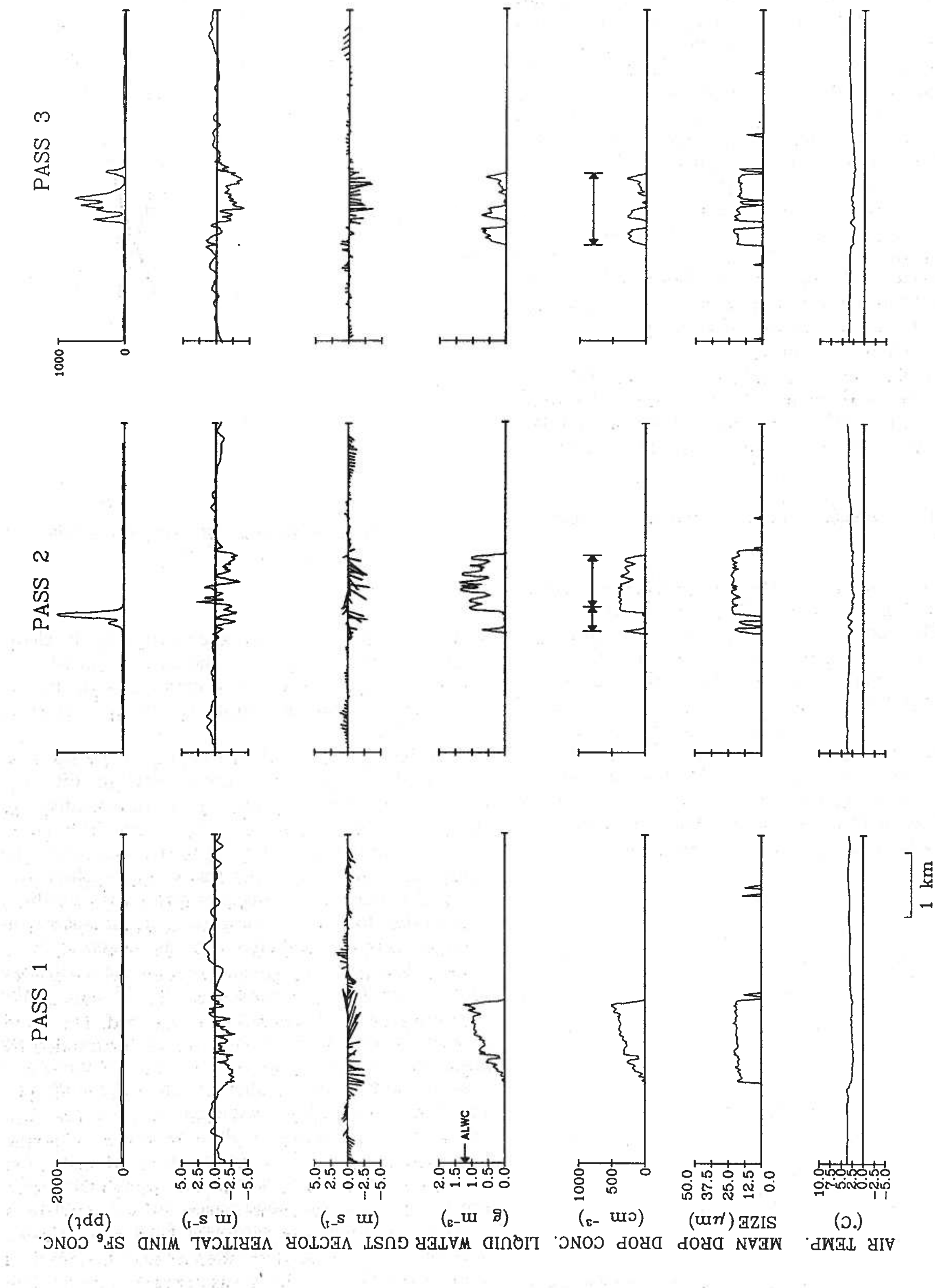

FIG. 15. As in Fig. 11 except for the small convective cloud on 11 August 1991. The regions marked by arrows above the droplet concentration were the regions selected for the droplet size spectra in Fig. 16.

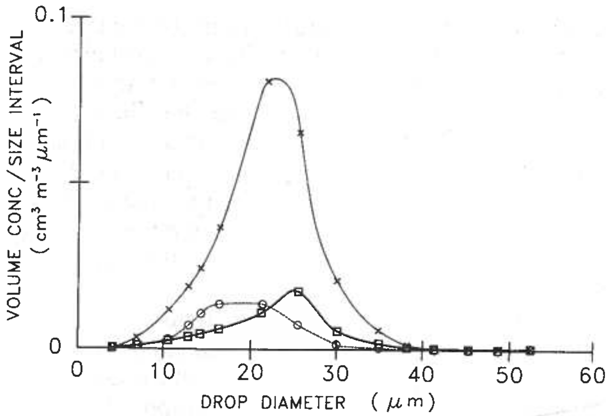

FIG. 16. Droplet volume size spectra for the main cloud region in Fig. 15, pass 2 (x), for the SF_6 region adjacent to it (boxes, heavy line) and in the mixed SF_6 region in pass 3 (circles, dashed line). These areas are marked in Fig. 15.

4. Evolution of the droplet size spectra during mixing

The smallest cloud described above was nonprecipitating and mixed the tracer through more than half of the cloud (Fig. 15, pass 2 and 3). The droplet size distributions before and after mixing are presented in Fig. 16. The spectra from three regions of the cloud were selected: the spectrum from the fragments of cloudy air in the tracer region on the edge of the turret during pass 2, the spectrum from the main cloud turret during pass 2, and the spectrum from the tracer region in pass 3 (after the tracer had mixed with the main turret). These regions are marked in Fig. 15.

The droplet spectrum from pass 2 in the center of the main turret contained a single narrow peak. The tracer region on the cloud edge had far fewer droplets, as expected, and the shape of the spectrum was depleted of small droplets compared to the main cloud. This suggests that the cloud on the edge was partially evaporated, since evaporation would have a greater effect on smaller droplet sizes. After the tracer had been entrained more fully into the main turret, the shape of the drop spectrum was similar to that found earlier in the main turret, except that the peak size was slightly smaller and fewer droplets overall were present. Evidently, the cloud from the edge of the turret did not provide enough larger drops to have much effect on the drop spectrum in the final mixture.

5. Discussion

For each of the clouds studied, the tracer was first found alongside of the treated turret before mixing into the central regions. This suggests that the circulation present near the cloud–air interface at the cloud top carries air from above the turret to the side of the cloud, where it is then entrained more fully into the cloud. This process is illustrated for the conditions observed on 22 June in Fig. 17. This type of circulation would be produced by a toroidal circulation of a growing cloud top, in accord with early studies of entraining thermals (e.g., Scorer 1958; Woodward 1959) or later revisions (Blyth et al. 1988, Fig. 18).

Scorer (1972) depicts the entrainment region just below the toroid, in accord with our observations, and a mixing region at the top. The latter region is called the entrainment region in the Blyth et al. model (see Fig. 18). However, the observations in section 3 indicate that the very top of the rising turret may be a region of comparatively shallow mixing. For example, the tracer region observed during pass 3 on 22 June was only about 300 m across (less than one-third of the size of the cloud, see Fig. 5) after about 8 min of transport and mixing since the release of the tracer above the cloud. (The tracer region was slightly more narrow than indicated in Fig. 6, due to the broadening caused by the 1-s response time of the analyzer.) During pass 4, 2 min later, the tracer had mixed horizontally

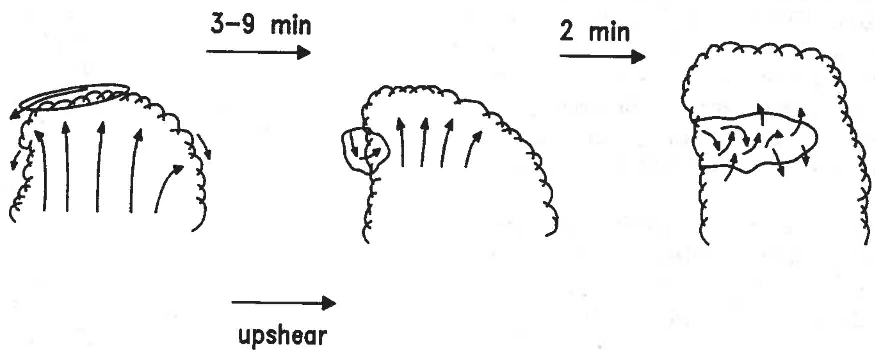

FIG. 17. Illustration of the suspected sequence of events that took place following the tracer release on 22 June 1989. During the first 3–9 min after the SF_6 release, part of the SF_6 was carried to the downshear/downwind side of the cloud in a narrow region on the cloud periphery, where it was entrained into the central cloud region by a small-scale vortex or eddy. During the next 2-min period, it rapidly mixed with the main cloud region. See the text for more details.

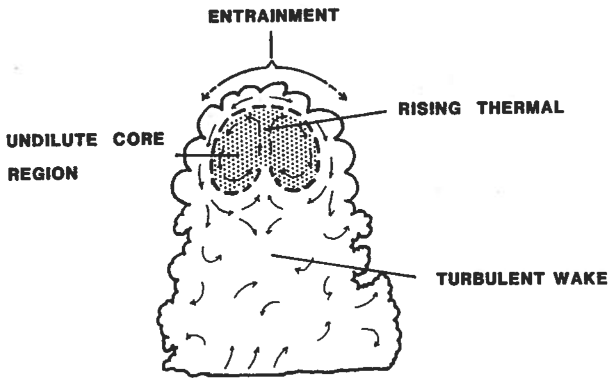

FIG. 18. Schematic shedding-thermal model of Blyth et al. Entrainment is depicted at the top of the cloud with an undiluted thermal shedding material in a turbulent wake. Diagram taken from Blyth et al. (1988).

through 1 km of the cloud (Fig. 7). Similar results are seen in the other cases (although the clouds were more short lived); in each case the tracer arrives at the side of the cloud turret before mixing with the main portion of the cloud. Fragments of cloud were found in and near the tracer regions on the side of the clouds (or at the midlevels of the cloud as in Fig. 5, pass 1), so some mixing and evaporation had likely taken place as the tracer was transported to the side of the cloud from the top. The droplet spectrum in Fig. 16 also suggests evaporation in the tracer region on the edge of the cloud.

Klaassen and Clark (1985) performed numerical experiments that showed a baroclinically driven instability of a laminar cloud top leads to the engulfment of discrete parcels of unsaturated air. This entrainment occurred via small nodes 100–200 m in size at the outer boundaries of their simulated cloud. They suggested, unlike the traditional concept of fluid diffusing across a turbulent interface, that a sharp (i.e., shallow) interface existed at the cloud top cased by a strong deformation flow near that region. The small vortex region observed on 22 June (Fig. 6, pass 3) appears similar to the nodes described above. The observations suggest that it did, in fact, entrain the tracer into the main body of the cloud in agreement with the original suggestion by Klaassen and Clark. Similar structures on the sides of a cloudy updraft are evident in other studies (e.g., Blyth et al. 1988).

Recently, Grabowski and Clark (1991) performed high-resolution numerical simulations of this process for a variety of conditions. They calculated the depth of the velocity tangential to the upper cloud interface as a function of the distance from the interface. These calculations were made for the interface region displaced a distance of 200 m from the cloud top along the periphery of the upper cloud interface. Their results are reproduced in Fig. 19. They indicate that the depth of significant tangential air movement near the upper cloud interface is on the order of tens of meters. This is too fine a resolution to be resolved by most airborne measurements. In the tracer experiments, this type of tangential movement would move the tracer to the sides of the cloud from its top as illustrated in Fig. 17. Such a shallow region of tangential velocity would carry the tracer in only a narrow ribbon from the top to the sides of the cloud. This may explain the narrow tracer regions that were first observed along the sides of the cloud turrets.

The mixing of dry air into the cloud top has been proposed as a possible means of broadening the droplet size distribution (Telford and Chai 1980). One of the steps in this chain is the preferential evaporation of the smallest droplets following entrainment of dry air into the cloud, followed by renewed lifting of the cloud, which allows surviving droplets to continue to grow by condensation. Telford and Chai showed that repeated cycles of this process could produce realistic droplet spectra. The results in section 4 show qualitatively the expected reduction in the small droplet sizes on the side of the cloud where some evaporation would be expected. However, the droplet spectra after mixing with the main cloud did not retain much of this effect, probably because of the much greater size of the main cloud. Repeated cycles of this process would be required to produce significant numbers of larger drops.

5. Summary

These studies are intended to lay the groundwork for future experiments. They demonstrate that airborne tracer release and sampling experiments are successful at observing the history of entrained air in cumuli.

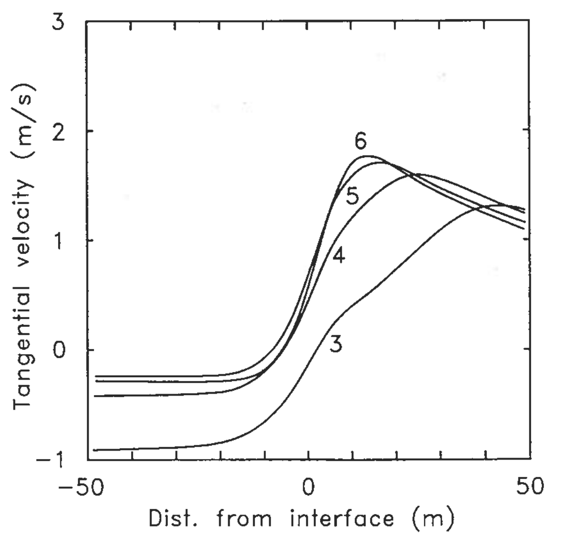

FIG. 19. Grabowski–Clark simulation of the velocity tangential to the cloud interface at a distance of 200 m from the cloud top along the periphery of the growing thermal. Curves are numbered according to time in minutes. The initial diameter of the thermal was 500 m. [Redrawn from Fig. 9 in Grabowski and Clark (1991)].

These types of experiments are useful for relating the entrainment process to other airborne cloud measurements such as droplet size or wind measurements. Although only a few observations are available to date, they offer supporting evidence for conceptual models of entrainment and the recent suggestions from the numerical simulations described above. However, more detailed comparisons between these types of experimental results with simulations of the cloud under investigation are needed. Comparisons with numerical simulations of parcel trajectories, such as the simulations in Reuter and Yau (1987), would also be useful.

The tracer technique offers opportunities for a variety of new experiments in cumuli. By employing a short-duration tracer release, it is possible to fix the time that air was at a given location in the cloud and to follow it in a Lagrangian frame of reference. This is a great help in constructing a history of the cloud. By releasing tracer outside the cloud, the history of entrained air can be studied. By releasing tracer at the cloud base the history of that air can be studied in a similar manner (Stith and Politovich 1989).

The main limitation of the tracer technique is the inability to adequately sample and map out the tracer concentrations with an aircraft. As with most in situ aircraft sampling, only a small and potentially unrepresentative portion of the region of interest is sampled by the aircraft. The best use of techniques such as these may be in combination with new remote-sensing methods for tracking air (e.g., Martner and Kropfli 1989). Experiments that utilize a combination of new techniques provide our best opportunity for developing a better understanding of entrainment and mixing in cumuli.

Acknowledgments. This work is supported by the NOAA Federal–State Cooperative Program in Atmospheric Modification Research, through NOAA cooperative agreement NA90AA-H-0A176 and Contract NDARB-UND-NOAA90 with the North Dakota Atmospheric Resource Board. Additional support was provided by the Environmental Protection Agency. Although the research described in this article has been funded wholly or in part by the United States Environmental Protection Agency through Cooperative Agreement CR-816010-01-0 to the University of North Dakota, it has not been subject to EPA review and therefore does not necessarily reflect the views of the EPA and no official endorsement should be inferred. Thanks are due to the many members of the field operations crew for making this study possible.

REFERENCES

Baumgardner, D., W. Strapp, and J. Dye, 1985: Evaluation of the forward scattering spectrometer probe. Part II: Corrections for coincidence and dead-time losses. *J. Atmos. Oceanic Technol.*, **2**, 626–632.

Benner, R. L., and B. Lamb, 1985: A fast response continuous analyzer for halogenated atmospheric tracers. *J. Atmos. Oceanic Technol.*, **2**, 582–589.

Blyth, A. M., W. A. Cooper, and J. B. Jensen, 1988: A study of the source of entrained air in Montana cumuli. *J. Atmos. Sci.*, **45**, 3944–3964.

Boatman, J. E., and A. H. Auer, 1983: The role of cloud top entrainment in cumulus clouds. *J. Atmos. Sci.*, **40**, 1517–1534.

Boe, B. A., J. L. Stith, P. L. Smith, J. H. Hirsch, J. H. Helsdon, Jr., A. G. Detwiler, H. D. Orville, B. E. Martner, R. F. Reinking, R. J. Metin, and R. A. Brown, 1992: The North Dakota Thunderstorm Project: A cooperative study of High Plains thunderstorms. *Bull. Amer. Meteor. Soc.*, **73**, 145–160.

Grabowski, W. W., and T. L. Clark, 1991: Cloud–environment interface instability: Rising thermal calculations in two spatial dimensions. *J. Atmos. Sci.*, **48**, 527–546.

Klaassen, G. P., and T. L. Clark, 1985: Dynamics of the cloud–environment interface and entrainment in small cumuli: Two-dimensional simulations in the absence of ambient shear. *J. Atmos. Sci.*, **42**, 2621–2642.

Lawson, R. P., and W. A. Cooper, 1990: Performance of some airborne thermometers in clouds. *J. Atmos. Oceanic Technol.*, **7**, 480–494.

Martner, B. E., and R. A. Kropfli, 1989: TRACIR: A radar technique for observing the exchange of air between clouds and their environment. *Atmos. Environ.*, **23**, 2715–2721.

Paluch, I. R., 1979: The entrainment mechanism in Colorado cumuli. *J. Atmos. Sci.*, **41**, 1801–1805.

Reuter, G. W., and M. K. Yau, 1987: Mixing mechanisms in cumulus congestus clouds. Part II: Numerical simulations. *J. Atmos. Sci.*, **44**, 798–827.

Scorer, R. S., 1958: *Natural Aerodynamics.* Pergamon, 312 pp.

——, 1972: *Clouds of the World.* Lothian, 176 pp.

Stith, J. L., and R. L. Benner, 1987: Applications of fast response continuous SF_6 analyzers to in situ cloud studies. *J. Atmos. Oceanic Technol.*, **4**, 599–619.

——, and M. K. Politovich, 1989: Observations of the effects of entrainment and mixing on the droplet size spectra in a small cumulus. *J. Atmos. Sci.*, **46**, 908–919.

——, A. G. Detwiler, R. F. Reinking, and P. L. Smith, 1990: Investigating transport, mixing and the formation of ice in cumuli with gaseous tracer techniques. *Atmos. Resch.*, **25**, 195–216.

Telford, J. W., and S. K. Chai, 1980: A new aspect of condensation theory. *Pure Appl. Geophys.*, **118**, 720–742.

Woodward, B., 1959: The motion in and around isolated thermals. *Quart. J. Roy. Meteor. Soc.*, **85**, 144–151.